Supporting Information for "$ClNO_2$ production from N_2O_5 uptake on saline playa dusts: New insights into potential inland sources of $ClNO_2$"

Dhruv Mitroo[1], Thomas E. Gill[2], Savannah Haas[3], Kerri A. Pratt[3], and Cassandra J. Gaston[1,*]

[1]Department of Atmospheric Sciences, Rosenstiel School of Marine & Atmospheric Sciences, University of Miami, Miami, FL 33149, USA

[2]Department of Geological Sciences and Environmental Science and Engineering Program, University of Texas at El Paso, El Paso, TX 79968, USA

[3]Department of Chemistry, University of Michigan, Ann Arbor, MI 48109, USA

[*]Corresponding Author: Email: cgaston@rsmas.miami.edu, Ph: (305) 421-4979

This Supporting Information (SI) contains: 13 pages, 5 figures, and 4 tables.

1. Playa Background Information

Black Rock Desert. The dominant minerals in the Black Rock Desert playa, in the western Great Basin of Nevada, are silicates (quartz, clay minerals and feldspars),[1,2] although a small fraction of evaporites and carbonates (e.g., NaCl and $CaCO_3$) have been measured.[2]

Great Salt Lake. The Great Salt Lake playa is located in the northeastern Great Basin in Utah. Unlike the Black Rock playa, the Great Salt Lake playa fringes are wet most of the year, and the surface sediments are predominantly evaporite salts.[3] Of these, the main salt observed is NaCl, with Br^- present at the ppm level.[4, 5]

Lordsburg. The Lordsburg playa is located in the northwestern Chihuahuan Desert of southwest New Mexico. Its surface sediments are not as salt-rich as other playas in this study; thus, it is likely more representative of the average Basin and Range playa geochemistry.[6] The sample used in this study was collected on the northern playa north of Interstate 10.

Salt Flat. The Salt Flat Basin is located in the northeastern Chihuahuan Desert in far west Texas. In addition to sodium chloride, its surface is rich in calcium sulfate (gypsum) and carbonates.[7]

Salton Sea. The Salton Sea, in the Colorado Desert of extreme south-central California, has been become more saline over time as its water supply, originally provided by a massive flood of the Colorado River, has for decades been provided only by (considerable) agricultural runoff, including pesticides, herbicides, and fertilizers.[8] Water conservation to restrict these agricultural wastewater flows has caused the Salton Sea to shrink and develop a saline playa, which is a potentially significant contributor to atmospheric dust. [9]

Sulphur Springs Draw. The lower part of the Sulphur Springs Draw, near its mouth in west-central Texas where the sample was collected, was within the basin of Pleistocene Lake Lomax.[10] The sample was collected in an area of numerous small playas in the draw (valley) bottom immediately downstream of the Natural Dam Salt Lake playa.[11-13] In addition to salt from naturally-occurring deposits, sediment at the Sulphur Springs Draw site also has been enriched in salinity by brine runoff from active and inactive oil and gas fields.[12, 13]

Dust Generation

Our setup uses a wrist-action shaker that agitates a custom-designed flask containing sediment samples, resulting in dust emission from the sediments. Once airborne, the dust is transported to a dilution drum. The dilution drum serves two functions: to impart energy (via cyclonic action) simulating natural dust emission through saltation/sandblasting, and to help smooth out spikes in aerosol concentrations. The resulting homogenized flow passes through a cyclone for selection of aerosol size range, and Po-210 strips for static elimination (thus reducing aerosol losses in the tubing). Finally, the flow is conditioned for humidity prior to delivery to the AFT. Flows are optimized for each sample (depending on sample 'sandiness') by regulating inlet flow to the conical flask holding the sample and flow through the dilution drum to give consistent aerosol concentration. A typical size distribution is thus lognormal and unimodal, as seen in Figure S4.

2. Chemical Ionization Mass Spectrometer (CIMS)

The instrument used for our study is identical to the one described by Kercher et al. (2009) and iodide (I^-) is used as the reagent ion.[14] Briefly, I^- was generated by introducing a flow of UHP N_2 across the headspace of a methyliodide (CH_3I) permeation tube through a ^{210}Po ionizer (NRD, LLC) that then enters the ion-molecule reaction (IMR) region axially to sample flow at a pressure of ~60 Torr. The CDC electric field strength was optimized to maximize throughput of $[I \cdot N_2O_5]^-$

and $[I \cdot ClNO_2]^-$ clusters and agreement with Kercher et al. (2009) was observed when using -20 V cm^{-1} field strength in the CDC. At this modest strength, we did not find any $ClNO_2$ detected as $[I \cdot Cl]^-$ clusters (e.g., Thornton and Abbatt (2005))[15], giving us confidence any $ClNO_2$ generated was fully monitored as $[I \cdot ClNO_2]^-$ clusters. N_2O_5, Cl_2, $ClNO_2$, Br_2, $BrNO_2$, and BrCl were all monitored online using this method. We calculate the sensitivity for N_2O_5 to be ~18 Hz ppt^{-1} for every MHz of total reagent ion signal (see the main article). We find a lower limit of detection of ~15 ppt for our instrument for both N_2O_5 and $ClNO_2$. For Br_2, we found that sensitivity varied as a function of RH with values typically in the range of 5-10 Hz ppt^{-1} for every MHz of total reagent ion signal, giving us a lower detection limit of ~23-45 ppt. The accuracy of the instrument is ~20%.[14]

Commercially available sodium chloride (NaCl) was used routinely throughout this study to generate aerosols of known reactivity with N_2O_5 that produce $ClNO_2$ with a yield of unity.[16] We ran experiments on NaCl using both the particle modulation, as well as the full decay technique, obtaining values for γ_{N2O5} and ϕ_{ClNO2} of 0.037 ± 0.002 and 1.2 ± 0.2, respectively, comparable to previous laboratory-based results.[15, 17-22] Note that our exceedance of unity yield is a result of experimental error (typically <25%, as reported by Kercher et al., 2009). We also used Arizona Test Dust (ATD; Ultrafine Mesh, Powder Technology, Inc.) to verify that non-playa dusts do not generate $ClNO_2$ and sodium bromide (NaBr) to characterize the brominated products and reactive uptake coefficient of N_2O_5 on NaBr.

3. Corrections to S

Corrections below are Equation (S1) for the SMPS and Equation (S2) for the APS:[23]

$$D_{ve} = \frac{D_m}{\chi} \quad \text{(S1)}$$

$$D_{ve} = D_a \sqrt{\frac{\rho_P}{\chi}} \quad \text{(S2)}$$

where D_{ve}, D_m, and D_a are the volume equivalent, mobility, and aerodynamic diameters, respectively; ρ_P is the aerosol density, and χ is the shape factor. For mineral dust, reported χ values range from ~1-1.25 (e.g., for Saharan dust)[24, 25] to ~1.36 (e.g., for quartz particles).[26] These corrections account for non-sphericity and the density of playa dusts, which are very important for the APS and only of minor importance for the SMPS since the SMPS never accounted for >7% of the observed surface area.

4. Ion Chromatography (IC)

Playa sediment extracts were prepared, described in Gaston et al. (2017),[27] by adding ~10 mg of crushed sediment to 30 mL nanopure water (>18 MΩ resistivity). Aliquots of the solutions were then sonicated at 60°C for 75 min for salt dissolution. The resulting suspension was filtered using a 0.22 μm syringe filter (Acrodisc, Pall Life Sciences) during injection into the ion chromatographs. Concentrations of soluble inorganic ions were measured using two different IC systems: for anions (Cl^-, NO_2^-, SO_4^{2-}, Br^-, NO_3^-, PO_4^{3-}), and cations (Na^+, NH_4^+, K^+, Mg^{2+}, Ca^{2+}). A Dionex ICS-1100 (for cations) and ICS-2100 (for anions) were used for analysis. Methanesulfonic acid (20 mM) was used as eluent for the cation column, and a KOH gradient generated by an EGC III KOH system was used as eluent for the anion column. All samples were run in triplicates. Sample blanks were obtained by filtering nanopure water in the absence of sediment grains and performing IC using the same method.

5. Example Photos of Sediment Samples and Locations Where Playa Sediments Were Collected

Figure S1: Owens Lake "crust" (left) and "sediment" (right) sample location. Photos by J.M. Nield and J. Lasser.

Figure S2: Locations of samples utilized for this study (stars).

Table S1: Geographical coordinates of playa samples utilized for this study.

Playa	Coordinates	U.S. County and State

	Lat	Long	
Black Rock Desert	40.697222	-119.334722	Pershing County NV
Great Salt Lake	40.772617	-112.159733	Salt Lake County UT
Lordsburg	32.277303	-108.888720	Hidalgo County NM
Owens Lake "salt crust"	36.387420	-117.954800	Inyo County CA
Owens Lake "sediment"	36.542170	-117.954600	
Salt Flat	31.787283	-104.972800	Hudspeth County TX
Salton Sea	33.515770	-115.936390	Riverside County CA
Sulphur Springs Draw	32.205506	-101.600203	Howard County TX

6. Playa Dust Generation Method

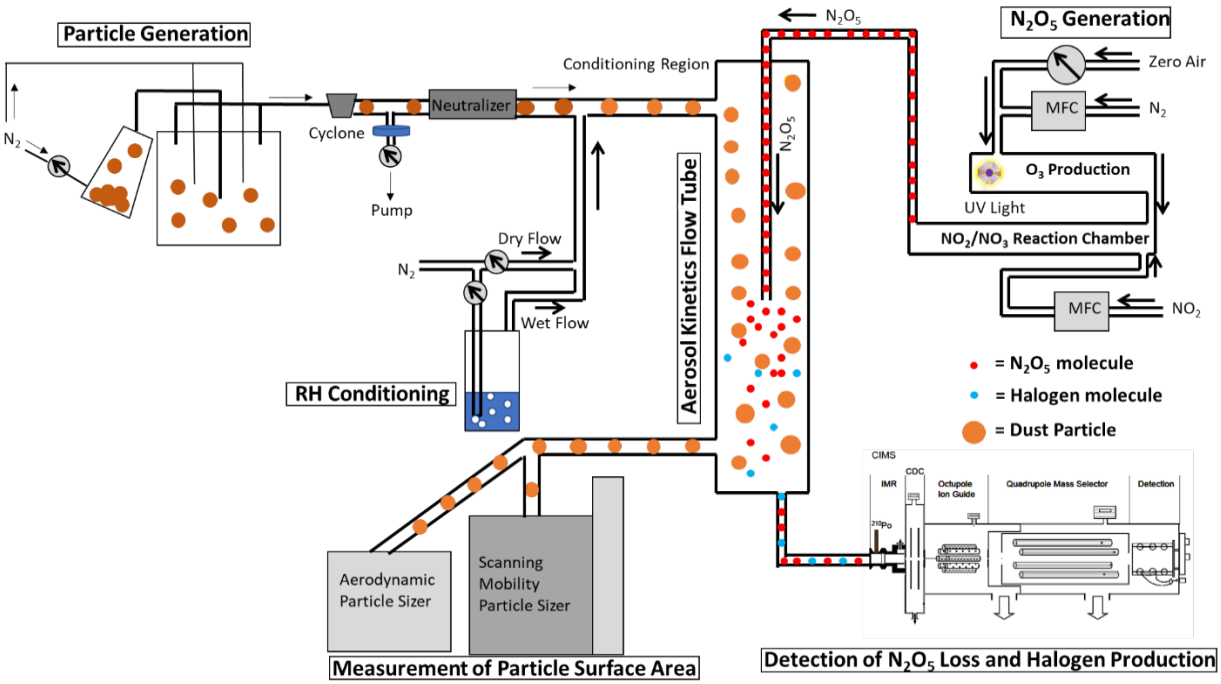

Figure S3: Experimental design.

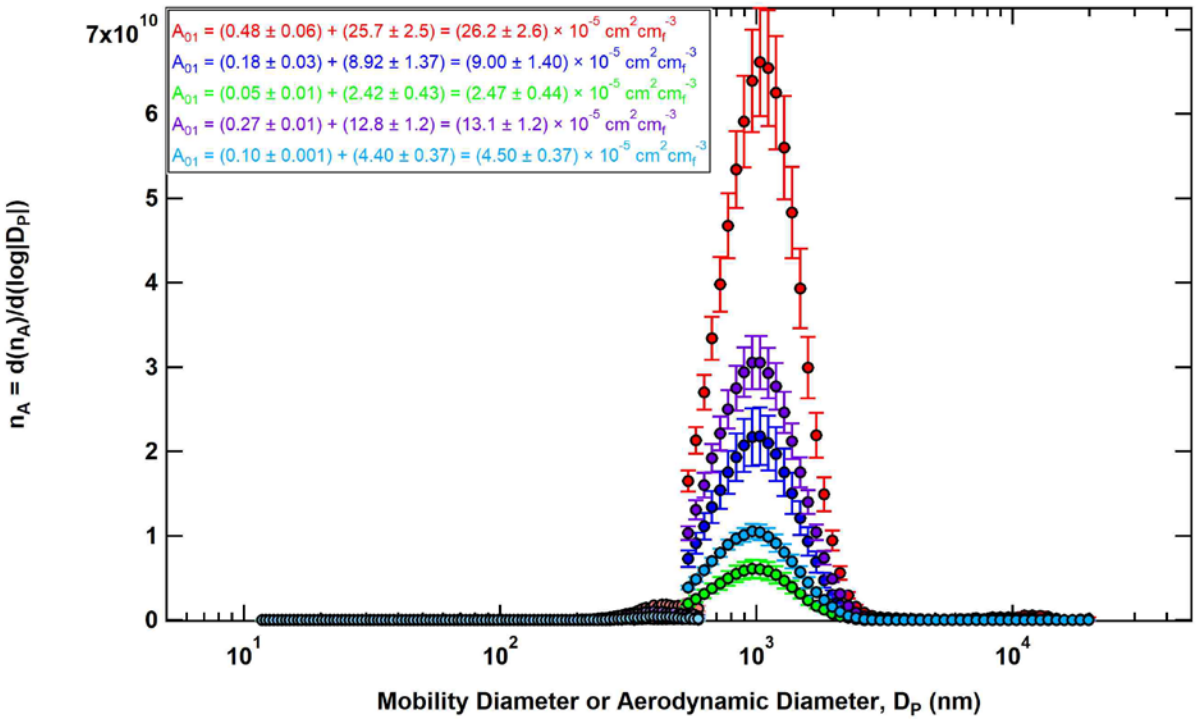

Figure S4: Typical aerosol size distribution from five repetitions during an experiment. Shown here is the aerosol size distribution for Lordsburg playa at 40% RH.

7. Reactive Uptake Measurements

For our experiments, we employed the particle modulation technique to determine γ_{N2O5} (see Section 2.3 in the Main Article); however, to ensure robust measurements, we employed both particle modulation and full decay technique for calibrations using pure deliquesced NaCl aerosols and obtained similar values. The advantage of the full decay is its robustness in determining k_{het} and k_{wall} by a multi-point process; however, it takes considerably longer than particle modulation. Further, particle modulation is more appropriate for our experiments with dust due to the stability of the particle surface area over long time periods. At a fixed injector position (resulting in a fixed mean residence time), we toggled aerosols on and off from the dust generation setup to the AFT. This method gives us two measurements that determine k_{het} (ΔN_2O_5) as well as $ClNO_2$ yield. We opted for this method instead of the full decay technique, where the injector position is varied throughout the experiment to obtain an $[N_2O_5]$ profile along the axial coordinate of the AFT, as it

is significantly faster. As shown by Bertram et al., 2009, both methods can be used to extract accurate values of γ_{N2O5}. To ensure its validity, that is, to ensure the reaction is of first order, we vary the surface area during repetitions to ensure k_{het} is linear with S, as seen in Figure S5, below.

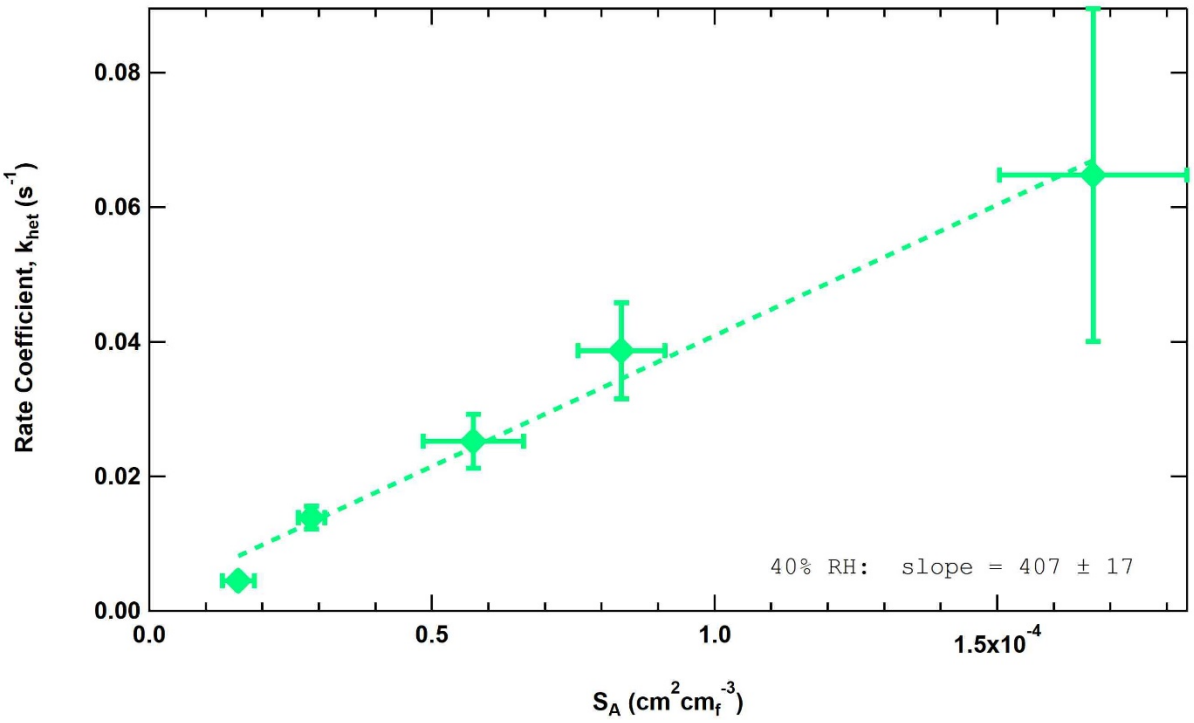

Figure S5: Linearity between heterogenous reaction rate constant and surface area concentration range for Lordsburg playa at 40% RH.

We also did attempt a decay experiment for one of our dust experiments and obtained similar values of k_{het} as we did when particle modulation was used; however, our standard deviation in k_{het} was significantly higher due to the instability of the particle surface area over the duration of the experiment.

Table S2: Aerosol measurement corrections.

Playa	Salt Fraction[a]	Correction to S	Correction to γ
Black Rock Desert	0.11	0.70	1.4
Great Salt Lake	0.49	0.79	1.3
Lordsburg	0.05	0.69	1.4

Owens Lake "crust"	0.68	0.85	1.2
Owens Lake "sediment"	0.17	0.71	1.4
Salt Flat	0.59	0.82	1.2
Salton Sea	0.49	0.79	1.3
Sulphur Springs Draw	0.11	0.70	1.4

[a]value estimated by IC data

Table S3: Measured values for reactive uptake coefficients (γ), the reactive uptake coefficient with a correction to the particle surface area (γ_{true}), and halogen yields (ϕ) for each playa sample and RH condition. Error bars represent $\pm 1\sigma$ of 5 repetitions at each RH.

Playa	**RH**	γ	γ_{true}	ϕ_{ClNO2}	ϕ_{Br2}
Black Rock Desert	29 ± 2	0.047 ± 0.003	0.072 ± 0.005	0.3 ± 0.1	-
	35 ± 2	0.042 ± 0.002	0.064 ± 0.003	0.54 ± 0.01	
	40 ± 2	0.027 ± 0.003	0.042 ± 0.005	0.6 ± 0.1	
	49 ± 1	0.014 ± 0.001	0.022 ± 0.002	0.58 ± 0.04	
Great Salt Lake	20 ± 1	0.006 ± 0.001	0.008 ± 0.001	0.8 ± 0.2	-
	30 ± 2	0.003 ± 0.002	0.004 ± 0.002	0.7 ± 0.2	
	51 ± 1	0.014 ± 0.003	0.019 ± 0.004	0.8 ± 0.1	
Lordsburg	21 ± 1	0.067 ± 0.025	0.105 ± 0.039	0.06 ± 0.02	-
	31 ± 1	0.049 ± 0.011	0.077 ± 0.017	0.05 ± 0.01	
	40 ± 1	0.050 ± 0.010	0.078 ± 0.016	0.08 ± 0.05	
	50 ± 1	0.079 ± 0.008	0.124 ± 0.012	0.08 ± 0.02	
Owens Lake "crust"	20 ± 2	0.007 ± 0.002	0.008 ± 0.002	0.46 ± 0.05	-
	31 ± 1	0.007 ± 0.002	0.009 ± 0.003	0.4 ± 0.1	
	40 ± 2	0.014 ± 0.004	0.017 ± 0.004	0.73 ± 0.08	
Owens Lake "sediment"	30 ± 2	0.054 ± 0.013	0.081 ± 0.020	0.60 ± 0.06	0.05 ± 0.01
	40 ± 2	0.042 ± 0.008	0.063 ± 0.011	0.75 ± 0.04	0.05 ± 0.02
	50 ± 2	0.044 ± 0.012	0.066 ± 0.018	0.6 ± 0.1	0.07 ± 0.03
Salt Flat	30 ± 1	0.016 ± 0.004	0.020 ± 0.005	1.0 ± 0.2	-
	40 ± 1	0.018 ± 0.008	0.022 ± 0.010	1.0 ± 0.3	
	50 ± 2	0.023 ± 0.005	0.028 ± 0.006	0.9 ± 0.3	
Salton Sea	16 ± 2	0.004 ± 0.002	0.006 ± 0.001	0.2 ± 0.1	-
	30 ± 2	0.003 ± 0.001	0.004 ± 0.001	0.7 ± 0.1	
	46 ± 2	0.004 ± 0.001	0.006 ± 0.001	0.7 ± 0.3	
Sulphur Springs Draw	30 ± 1	0.020 ± 0.006	0.030 ± 0.010	1.0 ± 0.2	-
	40 ± 2	0.019 ± 0.002	0.029 ± 0.003	1.2 ± 0.3	
	50 ± 2	0.028 ± 0.006	0.043 ± 0.009	0.8 ± 0.1	

Table S4: Inorganic soluble ion data. Values below the limit of detection are denoted as "BDL".

Sample	F^- (g/kg)		Cl^- (g/kg)		NO_2^- (g/kg)		SO_4^{2-} (g/kg)		Br^- (g/kg)		NO_3^- (g/kg)		PO_4^{3-} (g/kg)		Na^+ (g/kg)		NH_4^+ (g/kg)		K^+ (g/kg)		Mg^{2+} (g/kg)		Ca^{2+} (g/kg)	
	Mean	St. Dev	Mean	St. Dev	Mean	St. Dev	Mean	St. Dev	Mean	St. Dev	Mean	St. Dev	Mean	St. Dev	Mean	St. Dev	Mean	St. Dev	Mean	St. Dev	Mean	St. Dev	Mean	St. Dev
Black Rock Desert	1.2	0.5	40.1	0.4	0.2	0.04	1.9	0.09	0.4	0.03	1.1	0.06	0.6	0.2	38.9	0.3	BDL	BDL	2.6	0.03	0.6	0.02	24.6	1.7
Great Salt Lake	10.5	9.2	125.1	1.5	0.9	0.1	143.4	0.8	1.6	1.2	3.6	1.7	3.4	1.4	166.5	0.3	BDL	BDL	5.7	0.3	11.5	0.4	20.0	1.2
Lordsburg	4.7	2.9	0.6	0.2	0.2	0.1	0.5	0.4	0.9	0.5	1.6	0.8	1.4	0.7	7.6	0.2	1.1	0.4	0.9	0.1	0.7	0.06	31.4	7.0
Owens Lake "crust"	7.5	3.2	105.5	0.6	0.4	0.2	195.7	2.0	2.0	0.1	4.6	0.6	1.0	1.1	350.5	0.9	BDL	BDL	10.7	0.6	1.7	0.3	5.3	1.2
Owens Lake "sediment"	4.4	2.3	41.0	1.7	0.2	0.2	24.1	1.2	0.9	0.1	2.2	0.3	1.1	0.2	76.7	0.1	BDL	BDL	8.1	0.4	1.3	0.1	9.1	1.6
Salt Flat	2.9	1.4	88.4	0.1	0.5	0.06	252.9	0.4	0.7	0.0	1.6	0.2	0.3	0.1	58.8	0.5	BDL	BDL	2.7	0.08	8.4	1.4	171.8	5.3
Salton Sea	5.5	3.3	140.5	0.7	0.6	0.03	143.1	2.0	0.5	0.1	1.1	0.3	1.4	0.4	110.2	0.6	BDL	BDL	3.9	0.1	10.9	0.3	68.1	1.1
Sulphur Springs Draw	5.2	1.9	16.6	2.7	0.7	0.5	41.6	4.0	0.7	0.1	2.1	0.5	1.4	1.0	10.4	1.0	2.4	1.8	1.4	0.5	5.9	0.5	26.1	1.5

References

1. Gillies, J. A.; O'Connor, C. M.; Mamane, Y.; Gertler, A. W., Chemical profiles for characterizing dust sources in an urban area, western Nevada, USA *Zeitschrift fuer Geomorphologie* **1999,** *116*, 19-44.
2. Fantle, M. S.; Tollerud, H.; Eisenhauer, A.; Holmden, C., The Ca isotopic composition of dust-producing regions: Measurements of surface sediments in the Black Rock Desert, Nevada. *Geochim Cosmochim Ac* **2012,** *87*, 178-193.
3. Hahl, D. C.; Mitchell, C. G., Dissolved-mineral inflow to Great Salt Lake and chemical characteristics of Salt Lake brine - Part I: Selected Hydrologic Data. *Utah Geological and Mineralogical Survey Water-Resources Bulletin 3 - part 1* **1963**, 40.
4. Gwynn, J. W., Great Salt Lake, Utah: Chemical and physical variations of the brine and effects of the SPRR Causeway, 1966-1996. In *Modern and ancient lake systems : new problems and perspectives*, Pitman, J. K.; Carroll, A. R., Eds. Utah Geological Association Handbook: 1998; Vol. 26, pp 71-90.
5. Handy, A. H.; Hahl, D. C., Great Salt Lake-chemistry of the water. In *The Great Salt Lake*, Stokes, W. L., Ed. Utah Geological Survey Guidebook: 1966; Vol. 20, pp 135-151.
6. Scuderi, L. A.; Laudadio, C. K.; Fawcett, P. J., Monitoring playa lake inundation in the western United States: Modern analogues to late-Holocene lake level change. *Quaternary Res* **2010,** *73*, (1), 48-58.
7. Wilkins, D. E.; Currey, D. R., Timing and extent of late Quaternary paleolakes in the Trans-Pecos Closed Basin, west Texas and south-central New Mexico. *Quaternary Res* **1997,** *47*, (3), 306-315.
8. Arnal, R. E., Limnology, Sedimentation, and Microorganisms of the Salton Sea, California. *Geol Soc Am Bull* **1961,** *72*, (3), 427-478.
9. Frie, A. L.; Dingle, J. H.; Ying, S. C.; Bahreini, R., The Effect of a Receding Saline Lake (The Salton Sea) on Airborne Particulate Matter Composition. *Environ Sci Technol* **2017,** *51*, (15), 8283-8292.
10. Holliday, V. T., Stratigraphy and paleoenvironments of late Quaternary valley fills on the Southern High Plains. *Memoir of the Geological Society of America* **1995,** *186*, 136.
11. Frederick, C. D., Late Quaternary clay dune sedimentation on the Llano Estacado, Texas. *Plains Anthropol* **1998,** *43*, (164), 137-155.
12. Raines, T. H.; Rast, W., Characterization and simulation of the quantity and quality of water in the Highland Lakes, Texas, 1983-92. *U.S. Geological Survey Water Resources Investigation Report 99-4087* **1999**.
13. Slade, R. M.; Buszka, P. M., Characteristic of streams and aquifers and processes affecting the salinity of water in the upper Colorado River basin, Texas. *U.S. Geological Survey Water-Resources Investigations Report 94-4036* **1994**.
14. Kercher, J. P.; Riedel, T. P.; Thornton, J. A., Chlorine activation by N2O5: simultaneous, in situ detection of ClNO2 and N2O5 by chemical ionization mass spectrometry. *Atmos Meas Tech* **2009,** *2*, (1), 193-204.
15. Thornton, J. A.; Abbatt, J. P. D., N2O5 reaction on submicron sea salt aerosol: Kinetics, products, and the effect of surface active organics. *J Phys Chem A* **2005,** *109*, (44), 10004-10012.

16. Finlayson-Pitts, B. J.; Ezell, M. J.; Pitts Jr., J. N., Formation of chemically active chlorine compounds by reactions of atmospheric NaCl particles with gaseous N2O5 and ClONO2. *Nature* **1989,** *337*, 241-244.
17. Gaston, C. J.; Thornton, J. A., Reacto-Diffusive Length of N2O5 in Aqueous Sulfate- and Chloride-Containing Aerosol Particles. *J Phys Chem A* **2016,** *120*, (7), 1039-1045.
18. Behnke, W.; George, C.; Scheer, V.; Zetzsch, C., Production and decay of ClNO2, from the reaction of gaseous N2O5 with NaCl solution: Bulk and aerosol experiments. *J Geophys Res-Atmos* **1997,** *102*, (D3), 3795-3804.
19. McNeill, V. F.; Patterson, J.; Wolfe, G. M.; Thornton, J. A., The effect of varying levels of surfactant on the reactive uptake of N2O5 to aqueous aerosol. *Atmos Chem Phys* **2006,** *6*, 1635-1644.
20. Stewart, D. J.; Griffiths, P. T.; Cox, R. A., Reactive uptake coefficients for heterogeneous reaction of N2O5 with submicron aerosols of NaCl and natural sea salt. *Atmos Chem Phys* **2004,** *4*, 1381-1388.
21. Roberts, J. M.; Osthoff, H. D.; Brown, S. S.; Ravishankara, A. R.; Coffman, D.; Quinn, P.; Bates, T., Laboratory studies of products of N2O5 uptake on Cl- containing substrates. *Geophys Res Lett* **2009,** *36*, L20808.
22. Ryder, O. S.; Campbell, N. R.; Shaloski, M.; Al-Mashat, H.; Nathanson, G. M.; Bertram, T. H., Role of Organics in Regulating ClNO2 Production at the Air-Sea Interface. *J Phys Chem A* **2015,** *119*, (31), 8519-8526.
23. DeCarlo, P. F.; Slowik, J. G.; Worsnop, D. R.; Davidovits, P.; Jimenez, J. L., Particle morphology and density characterization by combined mobility and aerodynamic diameter measurements. Part 1: Theory. *Aerosol Sci Tech* **2004,** *38*, (12), 1185-1205.
24. Denjean, C.; Cassola, F.; Mazzino, A.; Triquet, S.; Chevaillier, S.; Grand, N.; Bourrianne, T.; Momboisse, G.; Sellegri, K.; Schwarzenbock, A.; Freney, E.; Mallet, M.; Formenti, P., Size distribution and optical properties of mineral dust aerosols transported in the western Mediterranean. *Atmos Chem Phys* **2016,** *16*, (2), 1081-1104.
25. Kaaden, N.; Massling, A.; Schladitz, A.; Muller, T.; Kandler, K.; Schutz, L.; Weinzierl, B.; Petzold, A.; Tesche, M.; Leinert, S.; Deutscher, C.; Ebert, M.; Weinbruch, S.; Wiedensohler, A., State of mixing, shape factor, number size distribution, and hygroscopic growth of the Saharan anthropogenic and mineral dust aerosol at Tinfou, Morocco. *Tellus B* **2009,** *61*, (1), 51-63.
26. Wagner, C.; Hanisch, F.; Holmes, N.; de Coninck, H.; Schuster, G.; Crowley, J. N., The interaction of N2O5 with mineral dust: aerosol flow tube and Knudsen reactor studies. *Atmos Chem Phys* **2008,** *8*, (1), 91-109.
27. Gaston, C. J.; Pratt, K. A.; Suski, K. J.; May, N. W.; Gill, T. E.; Prather, K. A., Laboratory Studies of the Cloud Droplet Activation Properties and Corresponding Chemistry of Saline Playa Dust. *Environ Sci Technol* **2017,** *51*, (3), 1348-1356.